Search for the gamma-ray spectral lines with the DAMPE and the Fermi-LAT observations

Ji-Gui Cheng,[1,2] Yun-Feng Liang,[1,*] and En-Wei Liang[1,†]

[1]*Guangxi Key Laboratory for Relativistic Astrophysics, School of Physical Science and Technology, Guangxi University, Nanning 530004, China*

[2]*School of Physics and Electronics, Hunan University of Science and Technology, Xiangtan 411201, China*

(Received 30 December 2022; revised 4 May 2023; accepted 18 August 2023; published 11 September 2023)

Weakly interacting massive particles, as a major candidate of dark matter (DM), may directly annihilate or decay into high-energy photons, producing monochromatic spectral lines in the gamma-ray band. These spectral lines, if detected, are smoking-gun signatures for the existence of new physics. Using the 5 years of Dark Matter Particle Explorer (DAMPE) data and 13 years of Fermi Large Area Telescope (Fermi-LAT) data, we search for linelike signals in the energy range of 3 GeV–1 TeV from the Galactic Halo. Different regions of interest are considered to accommodate different DM density profiles. We do not find any significant line structure, and the previously reported linelike feature at ∼133 GeV is also not detected in our analysis. Adopting a local DM density of $\rho_{\rm local} = 0.4\ {\rm GeV\,cm^{-3}}$, we derive 95% confidence level constraints on the velocity-averaged cross section of $\langle\sigma v\rangle_{\gamma\gamma} \lesssim 4\times10^{-28}\ {\rm cm^3\,s^{-1}}$ and the decay lifetime of $\tau_{\gamma\nu} \gtrsim 5\times10^{29}$ s at 100 GeV, achieving the strongest constraints to date for the line energies of 6–660 GeV. The improvement stems from the longer Fermi-LAT dataset used and the inclusion of DAMPE data in the analysis. The simultaneous use of two independent datasets could also reduce the systematic uncertainty of the search.

DOI: 10.1103/PhysRevD.108.063015

I. INTRODUCTION

Dark matter (DM) [1,2] dominates the matter component in the Universe. As suggested by the cosmic microwave background anisotropies, DM energy density is ∼6.4 times that of baryon [3]. Despite being abundant in the Universe, the nature of DM remains unknown. Many DM candidates have been proposed theoretically [4]. As one group of the most widely studied DM candidates, weakly interacting massive particles (WIMPs) can be found in many particle physics theories [5]. They may produce monochromatic spectral lines in the gamma-ray band via annihilation or decay, e.g., $\chi\chi\to\gamma\gamma$ of supersymmetric particles [6] and $\chi\to\gamma\nu$ of gravitinos [7]. Normal astrophysical processes are not expected to produce such sharp spectral lines. Therefore, the detection of line signals would be a smoking-gun signature for the existence of WIMPs.

Many research works have been carried out to search for spectral lines using gamma-ray observations from the Energetic Gamma-Ray Experiment Telescope, Fermi Large Area Telescope (Fermi-LAT), Dark Matter Particle Explorer (DAMPE), HESS, and MAGIC [8–29]. Among these works, several line candidates were temporarily reported, such as the ∼133 GeV line signals detected from the Galactic Center and galaxy clusters [11–17] and the ∼43 GeV tentative line signal found in the joint analysis of 16 nearby galaxy clusters [20,26]. However, these line candidates are absent in the subsequent searches or do not have large enough significance [19,26,27]. So far, no robust detection of a gamma-ray line has been claimed. Consequently, upper limits on the velocity-averaged cross section $\langle\sigma v\rangle_{\gamma\gamma}$ and lower limits on the decay lifetime $\tau_{\gamma\nu}$ are placed for WIMPs. As reported in [19], constraints of $\langle\sigma v\rangle_{\gamma\gamma} \lesssim 10^{-26}\ {\rm cm^3\,s^{-1}}$ and $\tau_{\gamma\nu} \gtrsim 10^{28}$ s at 100 GeV can be derived from the 5.8-yr Fermi-LAT observation of the Galactic Halo.

Similarly, the DAMPE Collaboration has conducted a systematic search for linelike signals targeting the Galactic Halo region with five years of accumulated data [27]. DAMPE is very suitable for searching for sharp gamma-ray structures in the GeV–TeV range. It has an excellent energy resolution (∼1.0% at 100 GeV [30]), which helps reduce the systematic uncertainty associated with background modeling. Reference [27] has shown that, although having a much smaller effective area, the constraints on the DM parameters of producing gamma-ray lines based on DAMPE observations are comparable to that of [19].

*liangyf@gxu.edu.cn
†lew@gxu.edu.cn

Inspired by the previous studies, in this paper, we analyze the 5 years of DAMPE [31] and 13 years of Fermi-LAT [32] publicly available data from the Galactic Halo to perform the line signal searches. The improvements of this work with respect to previous studies include the following: (1) we update the previous Fermi-LAT analysis (5.8 yr) with a longer dataset (13 yr); (2) we perform searches for line signals with the DAMPE and Fermi-LAT data jointly, which may reduce the uncertainties due to instrumental effects.

II. DATA REDUCTION

The Fermi-LAT is a wide field-of-view imaging gamma-ray telescope launched in 2008 [33]. So far, over 14 years of observation data have been accumulated. In this work, we analyze the Fermi-LAT PASS 8 data ranging from August 4, 2008 to September 24, 2021 (mission elapsed time: 239557417–654145676) to search for gamma-ray line signals. The latest (version 2.2.0) FERMITOOLS software is used to process the data in the energy range 3–1000 GeV. We use the instrument response functions P8R3_CLEAN_V3 and corresponding LAT events (evclass = 256 and evtype = 3) in our analysis. A maximum zenith angle of 100° is set to eliminate the contamination from the bright Earth limb. To ensure the data quality, the data quality cut (DATA_QUAL > 0) & & (LAT_CONFIC == 1) is applied.

We adopt four different regions of interest (ROIs) with radii of 16°, 40°, 86°, and 150° (denoted as R16, R40, R86, and R150, respectively) centering at the Sagittarius A* (right ascension, 266.415°; declination, −29.006°). The four ROIs are devised to optimize sensitivity for different DM density profiles [27]. Since the Galactic plane is expected to be dominated by standard astrophysical processes, the region of ($|l| < \Delta l$ and $|b| < 5°$) is masked from the ROIs to obtain a better line search sensitivity, where the Δl takes 5°, 9°, 0°, and 0° for R16, R40, R86, and R150, respectively [27]. We do not mask the photons from any detected point sources, since they only slightly affect the results (see Supplemental Material [34], Sec. A for details).

DAMPE is a space-based telescope launched in 2015 aiming to detect charged cosmic rays and gamma rays. It has great potential in searching for line signals owing to its excellent energy resolution [30]. In this work, we use five years of DAMPE publicly available data [31] (from January 1, 2016 to January 1, 2021) to perform the line signal search. The DmpST package [35] is employed to analyze the data. For DAMPE data, the same ROIs are adopted as that used in the Fermi-LAT data reduction. Events belonging to both the low- and high-energy triggers [35] in the energy range of 3 GeV–1 TeV are used. The events' incidence angles are restricted to $0.5 \leq \cos(\theta) \leq 1.0$ to ensure the data quality.

III. LIKELIHOOD FITTING

We perform an unbinned likelihood analysis in sliding energy windows to search for spectral lines [11,12,17–20]. The analysis procedure is briefly described below. We choose a series of line energies $E_{\rm line}$ with step lengths determined by the 68% instrument energy resolution σ_E. The window width is defined as $[0.5E_{\rm line}, 1.5E_{\rm line}]$. We ignore the energy windows with event counts $n_{\rm evt} < 30$ to guarantee sufficient statistics. Within each window, the maximum likelihood estimation is conducted by assuming a power-law background. The small width of the energy window warrants the power law is a good approximation to the background spectrum (see Supplemental Material [34], Sec. B for the spectra of the four ROIs). Effects caused by the power-law approximation will be corrected by a systematic uncertainty term in the likelihood (see below).

For the null and signal models, the log-likelihood functions are, respectively, written as

$$\ln \mathcal{L}_{\rm null}(\theta_{\rm b}) = \sum_{i=1}^{N} \ln(F_{\rm b}(E_i;\theta_{\rm b})\bar{\epsilon}(E_i)) - \int F_{\rm b}(E;\theta_{\rm b})\bar{\epsilon}(E){\rm d}E \quad (1)$$

and

$$\ln \mathcal{L}_{\rm sig}(N_{\rm s}, E_{\rm line}, \theta_{\rm b}) = \sum_{i=1}^{N} \ln[(F_{\rm b}(E_i;\theta_{\rm b})\bar{\epsilon}(E_i)) + F_{\rm s}(E_i)\bar{\epsilon}(E_{\rm line})] - \int [F_{\rm b}(E;\theta_{\rm b})\bar{\epsilon}(E) + F_{\rm s}(E)\bar{\epsilon}(E_{\rm line})]{\rm d}E. \quad (2)$$

In the above equations, E_i is the energy of each detected photon, $F_{\rm b}$ is the background flux, $F_{\rm s}$ is the line component expressed as $F_{\rm s} = N_{\rm s}\bar{D}(E;E_{\rm line})$, with $\bar{D}(E;E_{\rm line})$ the exposure-averaged instrument energy dispersion, and $\bar{\epsilon}$ is the average instrument exposure over the ROI. For details of our calculation of the energy dispersion $\bar{D}(E;E_{\rm line})$, please see Refs. [20,28] for the Fermi-LAT and DAMPE, respectively. The $\theta_{\rm b}$ represents the nuisance parameters of the background. For a joint analysis of multiple datasets, the joint log-likelihood is the sum of individual log-likelihood values of each dataset,

$$\ln \mathcal{L}_{\rm joint}(N_{\rm s}, E_{\rm line}, \theta_{\rm b,1}, \theta_{\rm b,2}) = \ln \mathcal{L}_{\rm F}(N_{\rm s}, E_{\rm line}, \theta_{\rm b,1}) + \ln \mathcal{L}_{\rm D}(N_{\rm s}, E_{\rm line}, \theta_{\rm b,2}). \quad (3)$$

During the analysis, the fitting is implemented by the PYTHON package IMINUIT [36].

The local significance of a line signal can be approximated as the square root of the test statistic (TS) value, where ${\rm TS} \triangleq 2(\ln \mathcal{L}_{\rm sig} - \ln \mathcal{L}_{\rm null})$. If no signal with TS > 25 is found, the upper limit of $N_{\rm sig}$ can be derived by varying the best-fit log-likelihood value $\ln\mathcal{L}_{\rm sig}$ by 1.35.

It has been discussed that systematic uncertainties may induce a false line signal or mask a true one in the fitting [17]. To account for such uncertainties, we adopt the same methodology as in [19] to reform the likelihood equations. By replacing $N_{\rm s}$ with $N_{\rm sys}+N_{\rm sig}$, the systematic uncertainty term

$$\ln\mathcal{L}_{\rm sys}(n_{\rm sys}) = \ln\left(\frac{1}{\sqrt{2\pi}\sigma_{\rm sys}}e^{-n_{\rm sys}^2/2\sigma_{\rm sys}^2}\right) \tag{4}$$

is added into Eqs. (1) and (2). In the above equation, the fractional signal is defined as $f \equiv n_{\rm sig}/b_{\rm eff}$ so that $\delta f_{\rm sys}$ can be obtained in the fitting of control regions ($\delta f_{\rm sys} \lesssim 1.5\%$ or 2.0% for the Fermi-LAT and the DAMPE, respectively, referring to [19,27]), and the effective background $b_{\rm eff}$ is the number of background photon counts under the signal peak [19]. More details on the effective background and the fitting of control regions are given in Supplemental Material [34], Secs. C and D, respectively.

IV. PREDICTED FLUX OF DM SPECTRAL LINE

Following previous studies of line signal searches [19,27], we consider three commonly used DM density profiles, which are (1) the Navarro-Frenk-White (NFW) profile [37]

$$\rho_{\rm NFW}(r) = \frac{\rho_{\rm s}}{(r/r_{\rm s})(1+r/r_{\rm s})^2}, \tag{5}$$

with $r_{\rm s} = 20$ kpc; (2) the Einasto profile [38,39]

$$\rho_{\rm Ein}(r) = \rho_{\rm s}\exp\{-(2/\alpha)[(r/r_{\rm s})^\alpha - 1]\}, \tag{6}$$

with $r_{\rm s} = 20$ kpc and $\alpha = 0.17$; and (3) the isothermal profile [40]

$$\rho_{\rm iso}(r) = \frac{\rho_{\rm s}}{1+(r/r_{\rm s})^2}, \tag{7}$$

with $r_{\rm s} = 5$ kpc. The local DM density $\rho_{\rm local}$ is set to $\rho_{\rm DM}(R_0) = 0.4\ {\rm GeV\,cm^{-3}}$ with $R_0 = 8.5$ kpc. Note that this value of $\rho_{\rm local}$ is intermediate among the ones reported in the literature [41]. A higher or lower value would strengthen or weaken the constraints on the DM parameters.

For each DM density profile, the J factor and D factor are calculated through $J_{\rm DM} = \int_{\rm ROI} d\Omega \int dl \rho_{\rm DM}^2$ and $D_{\rm DM} = \int_{\rm ROI} d\Omega \int dl \rho_{\rm DM}$, respectively. The ROIs and the J/D factors are paired into (R16, $J_{\rm Ein}$), (R40, $J_{\rm NFW}$), (R86, $J_{\rm iso}$), and (R150, $D_{\rm NFW}$) with corresponding values referring to Table 1 of Ref. [27].

The expected flux from DM annihilation $\chi\chi \to \gamma\gamma$ is expressed as

$$S_{\rm line}(E) = \frac{1}{4\pi}\frac{\langle\sigma v\rangle_{\gamma\gamma}}{2m_\chi^2}2\delta(E-E_{\rm line}) \times J_{\rm DM} = N_{\rm sig}\delta(E-E_{\rm line}), \tag{8}$$

in which $\langle\sigma v\rangle_{\gamma\gamma}$ is the velocity-averaged annihilation cross section, m_χ is the DM mass, and the energy of line photons is $E_{\rm line} = m_\chi$. The expected flux from DM decay $\chi \to \gamma\nu$ is given by

$$S_{\rm line}(E) = \frac{1}{4\pi}\frac{1}{m_\chi\tau_{\gamma\nu}}\delta(E-E_{\rm line}) \times D_{\rm DM} = N_{\rm sig}\delta(E-E_{\rm line}), \tag{9}$$

where $\tau_{\gamma\nu}$ is the decay lifetime, and the energy of the line signal is $E_{\rm line} = m_\chi/2$.

V. RESULTS AND DISCUSSION

Assuming DM annihilates or decays through $\chi\chi \to \gamma\gamma$ and $\chi \to \gamma\nu$ channels, respectively, we perform line searches with the DAMPE and the Fermi-LAT data. The search results of our joint analysis of DAMPE and Fermi data are shown in Fig. 1, where we show the TS values of potential line signals as a function of the line energy for the four selected ROIs. In total, there are 721 energy windows according to DAMPE's energy resolution in the energy range from 3 to 1000 GeV. In these windows, we find that no line signals have TS > 25 (corresponding to a local significance of $\gtrsim 5\sigma$) for the DM mass range from $m_\chi \sim 6$ to 660 GeV.[1] For R86 and R150, the highest TS values are $\lesssim$10, while for R16 and R40, the highest TS is merely ~6. The previously reported tentative line signal at ~133 GeV is not favored by the current joint analysis.

Since no line signal is found, we derive upper limits on $N_{\rm sig}$, and then convert them into the upper limits on $\langle\sigma v\rangle_{\gamma\gamma}$ or lower limits on $\tau_{\gamma\nu}$ via Eqs. (8) and (9), respectively. As is shown in Fig. 2, the five years of DAMPE data lead to constraints of $\langle\sigma v\rangle_{\gamma\gamma} \lesssim 9.0\times10^{-26}\ {\rm cm^3\,s^{-1}}$ and $\tau_{\gamma\nu} \gtrsim 3.0\times10^{28}$ s at $m_\chi = 100$ GeV (denoted as D5), consistent with the previous results by the DAMPE Collaboration [27]. Constraints derived from the 13 years of Fermi-LAT data (denoted as F13), on the other hand, are generally stronger than the D5 results, $\langle\sigma v\rangle_{\gamma\gamma,100\,{\rm GeV}} \lesssim 5.0\times10^{-27}\ {\rm cm^3\,s^{-1}}$ and $\tau_{\gamma\nu,100\,{\rm GeV}} \gtrsim 5.0\times10^{30}$ s. We note that the constraints from the joint analysis of the Fermi-LAT and DAMPE data (black line) are influenced by both the Fermi-LAT and DAMPE data and are stronger than both single constraints. Also, the joint constraints are more stringent than those from the 5.8 yrs of Fermi-LAT data [19] (denoted as F5.8) and the five years of DAMPE

[1]The range is a little narrower than that of our entire datasets (i.e., 3–1000 GeV) to allow for the spectral sidebands.

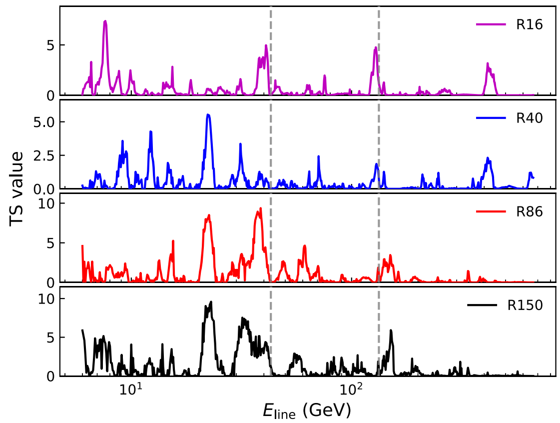

FIG. 1. TS values of putative gamma-ray lines as a function of line energies obtained in the joint likelihood analysis. From top to bottom, the panels are for 16°, 40°, 86°, and 150° ROIs centered on the Galactic Center, respectively. No line candidate is found with $\mathrm{TS_{joint}} > 25$. The two vertical dashed lines represent the tentative line signals at ∼43 [20] and ∼133 GeV [11,12], respectively.

data [27]. Our joint analysis, therefore, places the currently strongest constraints on gamma-ray lines from DM at 6–660 GeV energies to date.

The above results have accounted for systematic uncertainties by including an additional Gaussian term [Eq. (4)] in the likelihood. Figure 3 presents the results that ignore the systematic uncertainties, which can help us to understand the contributions of the two datasets in the joint analysis. It can be seen that the inclusion of systematic uncertainty prevents the Fermi-LAT results from improving with the data accumulation at the low-energy end. This is reasonable, because when the photon statistics is high enough, the detection sensitivity is dominated by the systematic uncertainty and will not change with the accumulation of data (see Supplemental Material [34], Sec. E for a detailed discussion). In contrast, although the DAMPE data are statistically subdominant, including DAMPE data can effectively reduce the sensitivity loss owing to the consideration of systematic uncertainty because of its better energy resolution.

To further validate the improved results achieved through better energy resolution, we conduct tests using the

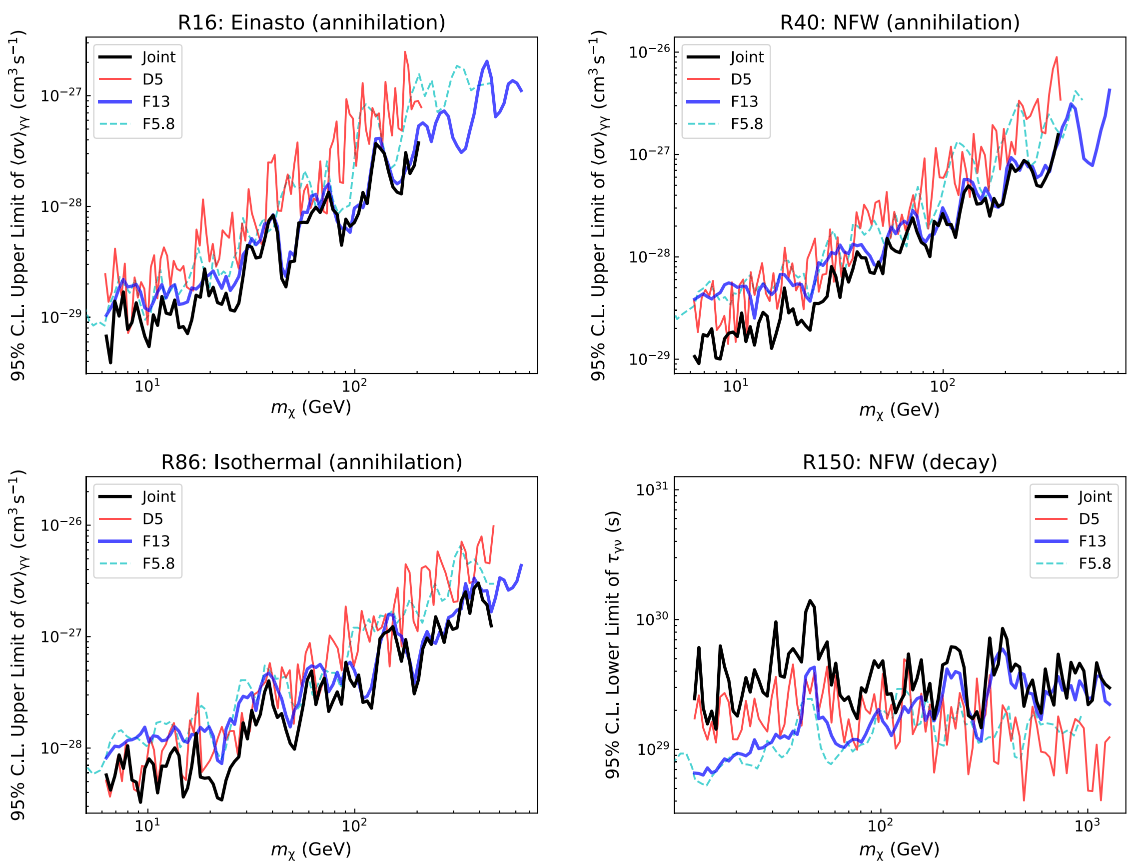

FIG. 2. The 95% confidence level constraints on $\langle\sigma v\rangle_{\gamma\gamma}$ and $\tau_{\gamma\nu}$ for different ROIs and DM density profiles. The D5 and F13 are the constraints based on 5 years of DAMPE data and 13 years of Fermi-LAT data, respectively. The joint constraints are derived by combining the likelihood of D5 and F13 in the unbinned likelihood analysis. The limits reported in [19] based on 5.8 yrs of Fermi-LAT data are also shown for comparison (denoted as F5.8).

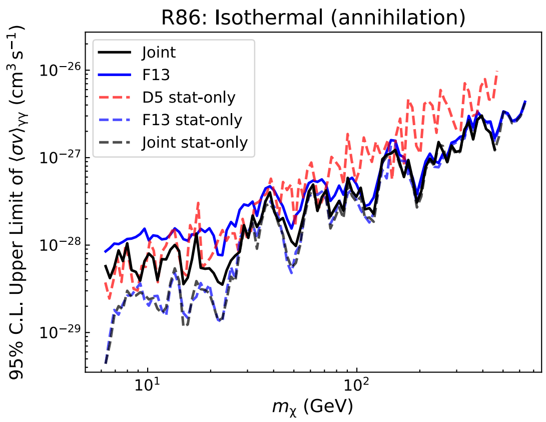

FIG. 3. Constraints on $\langle\sigma v\rangle_{\gamma\gamma}$ from the analysis *ignoring* systematic uncertainties and comparisons to our nominal results, which take systematic effects into account. Only the results of the R86 ROI are shown here as a demonstration; see Supplemental Material [34], Sec. G for other ROIs.

EDISP3 data of Fermi-LAT (a subgroup of data that have the best energy reconstruction quality, see Supplemental Material [34], Sec. F for details) to derive the constraints. We find that, in the low-energy range, better results are obtained from the EDISP3 analysis, indicating the better energy resolution [which reduces $b_{\rm eff}$ and $\delta f_{\rm sys}$ in Eq. (4)] does help to improve the analysis results. In the high-energy range, the EDISP3 constraints are slightly weaker than our nominal results because the EDISP3 data lose $3/4$ of the statistics. Note that this paper does not separately consider the four EDISP event types of Fermi-LAT data to perform a summed likelihood analysis. If so, the good energy resolution of EDISP3 can be utilized without loss of statistics, and the results could be further improved. Previous analyses pointed out that it could improve $\sim$15% for the Fermi-LAT only analysis [17,19].

This work combines the DAMPE and Fermi-LAT data to perform spectral line searches, which to our knowledge is the first work that combines data from different gamma-ray detectors to search for DM signals. Although the 130 GeV tentative signal is not supported by subsequent analyses [19,27,42], the approach we show here is not limited to the searches of spectral lines. Our work reveals the great potential of combining different instruments in improving the sensitivity of DM indirect search, demonstrating a new means to enhance the sensitivity. In the future, with more and more gamma-ray detectors (such as HERD [43] and VLAST [44]) starting observations, and with the increasing accumulation of Fermi-LAT and DAMPE data, such a joint analysis will become even more important.

VI. SUMMARY

In this work, we jointly analyze the Fermi-LAT and DAMPE data to search for linelike signals from the DM annihilation or decay in the Galactic Halo. Using the sliding energy window method and unbinned likelihood analysis, we find no evidence for a gamma-ray line having a local significance of $> 5\sigma$. Assuming DM particles annihilate through the $\chi\chi \to \gamma\gamma$ channel or decay through the $\chi \to \gamma\nu$ channel and adopting a local DM density of $\rho_{\rm local} = 0.4~{\rm GeV\,cm^{-3}}$, we derive the upper limits on $\langle\sigma v\rangle_{\gamma\gamma}$ and the lower limits on $\tau_{\gamma\nu}$ for different ROIs and DM density profiles. We improve the previous constraints on these parameters by a factor of $\sim\sqrt{2}$.

The improvement is due in part to the use of a larger Fermi-LAT dataset and in part to the combined analysis of data from two independent instruments. The simultaneous use of the Fermi-LAT and DAMPE data makes the obtained constraints stronger than the ones based on Fermi-LAT or DAMPE data alone. Further, since two independent instruments are employed, the systematic effects from individual instruments could also be reduced.

Although line signals are still absent and the constraints are getting more stringent, WIMP is still one of the most promising DM models. Recently, two experiments at Fermilab, E989 and CDF II, reported anomalies for muon anomalous magnetic moment $(g-2)$ [45] and W-boson mass [46], deviating from the prediction of the Standard Model by about 4.2σ and 7σ, respectively. Such results may indicate the existence of new physics and can be well explained by introducing WIMPs [47–49], which motivates us to keep searching for the annihilation or decay signals from WIMPs (e.g., gamma-ray lines).

The supporting data for this article are publicly available from [31,32].

ACKNOWLEDGMENTS

We thank Qiang Yuan, Yizhong Fan, and Zhaoqiang Shen for the helpful suggestions and discussions. We acknowledge data and software provided by the Fermi Science Support Center. We acknowledge data resources from Dark Matter Particle Explorer (DAMPE) satellite mission supported by Strategic Priority Program on Space Science and data service provided by National Space Science Data Center of China. This work is supported by the National Key Research and Development Program of China (No. 2022YFF0503304), the National Natural Science Foundation of China (No. 12133003) and the Guangxi Science Foundation (No. 2019AC20334).

[1] G. Jungman, M. Kamionkowski, and K. Griest, Supersymmetric dark matter, Phys. Rep. **267**, 195 (1996).
[2] G. Bertone, D. Hooper, and J. Silk, Particle dark matter: Evidence, candidates and constraints, Phys. Rep. **405**, 279 (2005).
[3] N. Aghanim *et al.*, Planck 2018 results. VI. Cosmological parameters, Astron. Astrophys. **641**, A6 (2020).
[4] B.-L. Young, A survey of dark matter and related topics in cosmology, Front. Phys. **12**, 121201 (2017).
[5] J. L. Feng, Dark matter candidates from particle physics and methods of detection, Annu. Rev. Astron. Astrophys. **48**, 495 (2010).
[6] L. Bergström and H. Snellman, Observable monochromatic photons from cosmic photino annihilation, Phys. Rev. D **37**, 3737 (1988).
[7] A. Ibarra and D. Tran, Gamma-Ray Spectrum from Gravitino Dark Matter Decay, Phys. Rev. Lett. **100**, 061301 (2008).
[8] A. R. Pullen, R.-R. Chary, and M. Kamionkowski, Search with EGRET for a gamma ray line from the Galactic Center, Phys. Rev. D **76**, 063006 (2007).
[9] A. A. Abdo *et al.*, Fermi Large Area Telescope Search for Photon Lines from 30 to 200 GeV and Dark Matter Implications, Phys. Rev. Lett. **104**, 091302 (2010).
[10] M. Ackermann *et al.*, Fermi LAT search for dark matter in gamma-ray lines and the inclusive photon spectrum, Phys. Rev. D **86**, 022002 (2012).
[11] T. Bringmann, X. Huang, A. Ibarra, S. Vogl, and C. Weniger, Fermi LAT search for internal bremsstrahlung signatures from dark matter annihilation, Annu. Rev. Astron. Astrophys. **2012**, 054 (2012).
[12] C. Weniger, A tentative gamma-ray line from dark matter annihilation at the Fermi Large Area Telescope, Annu. Rev. Astron. Astrophys. **2012**, 007 (2012).
[13] A. Geringer-Sameth and S. M. Koushiappas, Dark matter line search using a joint analysis of dwarf galaxies with the Fermi Gamma-ray Space Telescope, Phys. Rev. D **86**, 021302 (2012).
[14] X. Huang, Q. Yuan, P.-F. Yin, X.-J. Bi, and X. Chen, Constraints on the dark matter annihilation scenario of Fermi 130 GeV gamma-ray line emission by continuous gamma-rays, Milky Way halo, galaxy clusters and dwarf galaxies observations, Annu. Rev. Astron. Astrophys. **2012**, 048 (2012).
[15] E. Tempel, A. Hektor, and M. Raidal, Fermi 130 GeV gamma-ray excess and dark matter annihilation in subhaloes and in the Galactic centre, Annu. Rev. Astron. Astrophys. **2012**, 032 (2012).
[16] A. Hektor, M. Raidal, and E. Tempel, Evidence for indirect detection of dark matter from galaxy clusters in Fermi γ-ray data, Astrophys. J. Lett. **762**, L22 (2013).
[17] M. Ackermann *et al.*, Search for gamma-ray spectral lines with the Fermi Large Area Telescope and dark matter implications, Phys. Rev. D **88**, 082002 (2013).
[18] A. Albert, G. A. Gómez-Vargas, M. Grefe, C. Muñoz, C. Weniger, E. D. Bloom, E. Charles, M. N. Mazziotta, and A. Morselli, Search for 100 MeV to 10 GeV γ-ray lines in the Fermi-LAT data and implications for gravitino dark matter in the $\mu\nu$SSM, Annu. Rev. Astron. Astrophys. **2014**, 023 (2014).
[19] M. Ackermann *et al.*, Updated search for spectral lines from Galactic dark matter interactions with pass 8 data from the Fermi Large Area Telescope, Phys. Rev. D **91**, 122002 (2015).
[20] Y.-F. Liang, Z.-Q. Shen, X. Li, Y.-Z. Fan, X. Huang, S.-J. Lei, L. Feng, E.-W. Liang, and J. Chang, Search for a gamma-ray line feature from a group of nearby galaxy clusters with Fermi LAT Pass 8 data, Phys. Rev. D **93**, 103525 (2016).
[21] B. Anderson, S. Zimmer, J. Conrad, M. Gustafsson, M. Sánchez-Conde, and R. Caputo, Search for gamma-ray lines towards galaxy clusters with the Fermi-LAT, J. Cosmol. Astropart. Phys. 02 (2016) 026.
[22] H. Abdalla *et al.* (H.E.S.S. Collaboration), H.E.S.S. Limits on Linelike Dark Matter Signatures in the 100 GeV to 2 TeV Energy Range Close to the Galactic Center, Phys. Rev. Lett. **117**, 151302 (2016).
[23] H. Abdallah *et al.* (HESS Collaboration), Search for γ-Ray Line Signals from Dark Matter Annihilations in the Inner Galactic Halo from 10 Years of Observations with H.E.S.S., Phys. Rev. Lett. **120**, 201101 (2018).
[24] S. Li, Z.-Q. Xia, Y.-F. Liang, K.-K. Duan, Z.-Q. Shen, X. Li, L. Feng, Q. Yuan, Y.-Z. Fan, and J. Chang, Search for line-like signals in the all-sky Fermi-LAT data, Phys. Rev. D **99**, 123519 (2019).
[25] A. Albert *et al.* (HAWC Collaboration), Search for gamma-ray spectral lines from dark matter annihilation in dwarf galaxies with the High-Altitude Water Cherenkov observatory, Phys. Rev. D **101**, 103001 (2020).
[26] Z.-Q. Shen, Z.-Q. Xia, and Y.-Z. Fan, Search for line-like and box-shaped spectral features from nearby galaxy clusters with 11.4 years of Fermi Large Area Telescope data, Astrophys. J. **920**, 1 (2021).
[27] F. Alemanno *et al.* (DAMPE Collaboration), Search for gamma-ray spectral lines with the dark matter particle explorer, Sci. Bull. **67**, 679 (2022).
[28] T.-C. Liu, J.-G. Cheng, Y.-F. Liang, and E.-W. Liang, Search for gamma-ray line signals around the black hole at the Galactic Center with DAMPE observation, Sci. China Phys. Mech. Astron. **65**, 269512 (2022).
[29] MAGIC Collaboration, H. Abe *et al.*, Search for Gamma-Ray Spectral Lines from Dark Matter Annihilation up to 100 TeV toward the Galactic Center with MAGIC, Phys. Rev. Lett. **130**, 061002 (2023).
[30] J. Chang *et al.*, The dark matter particle explorer mission, Astropart. Phys. **95**, 6 (2017).
[31] The DAMPE data are available at https://dampe.nssdc.ac.cn/dampe/dataquerysc.php.
[32] The Fermi-LAT data are publicly available in the Fermi Science Support Center, https://fermi.gsfc.nasa.gov/ssc/data/access/.
[33] W. B. Atwood *et al.*, The Large Area Telescope on the Fermi gamma-ray space telescope mission, Astrophys. J. **697**, 1071 (2009).
[34] See Supplemental Material at http://link.aps.org/supplemental/10.1103/PhysRevD.108.063015 for some supplemental analyses, discussion, and figures.
[35] K.-K. Duan *et al.*, DmpIRFs and DmpST: DAMPE instrument response functions and science tools for gamma-ray data analysis, Res. Astron. Astrophys. **19**, 132 (2019).

[36] H. Dembinski *et al.*, scikit-hep/iminuit: v2.11.2, Zenodo (2022).
[37] J. F. Navarro, C. S. Frenk, and S. D. M. White, The structure of cold dark matter halos, Astrophys. J. **462**, 563 (1996).
[38] J. Einasto, On the construction of a composite model for the galaxy and on the determination of the system of galactic parameters, Tr. Astrofiz. Inst. Alma-Ata **5**, 87 (1965).
[39] J. F. Navarro, A. Ludlow, V. Springel, J. Wang, M. Vogelsberger, S. D. M. White, A. Jenkins, C. S. Frenk, and A. Helmi, The diversity and similarity of simulated cold dark matter haloes, Mon. Not. R. Astron. Soc. **402**, 21 (2010).
[40] J. N. Bahcall and R. M. Soneira, The universe at faint magnitudes. I. Models for the Galaxy and the predicted star counts., Astrophys. J. Suppl. Ser. **44**, 73 (1980).
[41] P. F. de Salas and A. Widmark, Dark matter local density determination: Recent observations and future prospects, Rep. Prog. Phys. **84**, 104901 (2021).
[42] D. P. Finkbeiner, M. Su, and C. Weniger, Is the 130 GeV line real? A search for systematics in the Fermi-LAT data, J. Cosmol. Astropart. Phys. 01 (2013) 029.
[43] X. Huang *et al.*, Perspective of monochromatic gamma-ray line detection with the High Energy Cosmic-Radiation Detection (HERD) facility onboard China's space station, Astropart. Phys. **78**, 35 (2016).
[44] Y. Z. Fan *et al.*, Very large area gamma-ray space telescope (VLAST), Acta Astronomica Sinica **63**, 27 (2022).
[45] B. Abi *et al.*, Measurement of the Positive Muon Anomalous Magnetic Moment to 0.46 ppm, Phys. Rev. Lett. **126**, 141801 (2021).
[46] T. Aaltonen *et al.* (CDF Collaboration), High-precision measurement of the W boson mass with the CDF II detector, Science **376**, 170 (2022).
[47] Y.-Z. Fan, T.-P. Tang, Y.-L. S. Tsai, and L. Wu, Inert Higgs Dark Matter for CDF II W-Boson Mass and Detection Prospects, Phys. Rev. Lett. **129**, 091802 (2022).
[48] G.-W. Yuan, L. Zu, L. Feng, Y.-F. Cai, and Y.-Z. Fan, Is the W-boson mass enhanced by the axion-like particle, dark photon, or chameleon dark energy?, Sci. China Phys. Mech. Astron. **65**, 129512 (2022).
[49] C.-R. Zhu, M.-Y. Cui, Z.-Q. Xia, Z.-H. Yu, X. Huang, Q. Yuan, and Y.-Z. Fan, Explaining the GeV Antiproton Excess, GeV γ-Ray Excess, and W-Boson Mass Anomaly in an Inert Two Higgs Doublet Model, Phys. Rev. Lett. **129**, 231101 (2022).